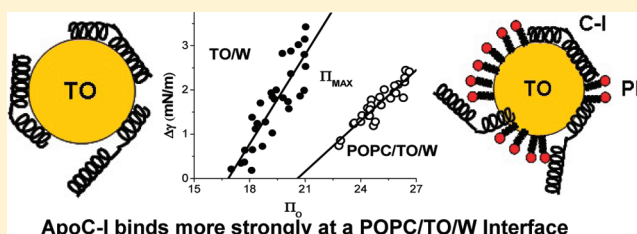


# Apolipoprotein C-I Binds More Strongly to Phospholipid/Triolein/Water than Triolein/Water Interfaces: A Possible Model for Inhibiting Cholesterol Ester Transfer Protein Activity and Triacylglycerol-Rich Lipoprotein Uptake

Nathan L. Meyers, Libo Wang, and Donald M. Small\*

Department of Physiology and Biophysics, Boston University School of Medicine, Boston, Massachusetts 02118, United States

**ABSTRACT:** Apolipoprotein C-I (apoC-I) is an important constituent of high-density lipoprotein (HDL) and is involved in the accumulation of cholesterol ester in nascent HDL via inhibition of cholesterol ester transfer protein and potential activation of lecithin:cholesterol acyltransferase (LCAT). As the smallest exchangeable apolipoprotein (57 residues), apoC-I transfers between lipoproteins via a lipid-binding motif of two amphipathic  $\alpha$ -helices (A $\alpha$ Hs), spanning residues 7–29 and 38–52. To understand apoC-I's behavior at hydrophobic lipoprotein surfaces, oil drop tensiometry was used to compare the binding to triolein/water (TO/W) and palmitoyl-oleoylphosphatidylcholine/triolein/water (POPC/TO/W) interfaces. When apoC-I binds to either interface, the surface tension ( $\gamma$ ) decreases by  $\sim 16$ – $18$  mN/m. ApoC-I can be exchanged at both interfaces, desorbing upon compression and readsorbing on expansion. The maximal surface pressures at which apoC-I begins to desorb ( $\Pi_{\text{max}}$ ) were 16.8 and 20.7 mN/m at TO/W and POPC/TO/W interfaces, respectively. This suggests that apoC-I interacts with POPC to increase its affinity for the interface. ApoC-I is more elastic on POPC/TO/W than TO/W interfaces, marked by higher values of the elasticity modulus ( $\epsilon$ ) on oscillations. At POPC/TO/W interfaces containing an increasing POPC:TO ratio, the pressure at which apoC-I begins to be ejected increases as the phospholipid surface concentration increases. The observed increase in apoC-I interface affinity due to higher degrees of apoC-I–POPC interactions may explain how apoC-I can displace larger apolipoproteins, such as apoE, from lipoproteins. These interactions allow apoC-I to remain bound to the interface at higher  $\Pi$  values, offering insight into apoC-I's rearrangement on triacylglycerol-rich lipoproteins as they undergo  $\Pi$  changes during lipoprotein maturation by plasma factors such as lipoprotein lipase.



Apolipoprotein C-I (apoC-I) is synthesized in the liver and circulates in the plasma bound to the surface of high-density lipoproteins (HDLs), very low-density lipoproteins (VLDLs), intermediate-density lipoproteins (IDLs), and chylomicrons.<sup>1</sup> As the smallest exchangeable apolipoprotein (57 amino acids), apoC-I transfers between lipoproteins and chylomicrons, altering their metabolic properties.<sup>2,3</sup> On nascent HDL, apoC-I is a potent activator of lecithin:cholesterol acyltransferase (LCAT), which allows for the accumulation of cholesterol ester (CE) and HDL particle maturation. ApoC-I serves as a secondary activator of LCAT, activating the enzyme with 10–45% efficacy relative to its primary activator, apolipoprotein A-I.<sup>4–6</sup> ApoC-I is a potent inhibitor of cholesterol ester transfer protein (CETP), which promotes exchange of CE and triacylglycerols (TAGs) between HDL and VLDL or LDL.<sup>7–9</sup> On the surface of HDL, apoC-I displaces hepatic lipase (HL), which hydrolyzes HDL phospholipids and mono- and diglycerides.<sup>10–12</sup> In activating LCAT and inhibiting CETP and HL, apoC-I aids in the synthesis and stabilization of mature HDL particles.

Comparatively, apoC-I is known to inhibit activity of lipoprotein lipase (LPL), an enzyme critical for hydrolysis of VLDL triacylglycerols and conversion of VLDL to LDL.<sup>13</sup>

ApoC-I further inhibits clearance of TAG-rich lipoproteins and their remnants by impairing interactions with the cellular receptors mediating their uptake.<sup>14,15</sup> Impaired uptake of  $\beta$ -VLDL has been linked to apoC-I-induced displacement of apoE, the ligand for the low-density lipoprotein receptor-related protein (LRP).<sup>16–18</sup> Together, these findings suggest that apoC-I lipoprotein surface modifications could displace apoE or HL, while the structure of apoC-I on the lipoprotein surface may allow for a portion of the peptide to interact with and regulate the function of LCAT or CETP. Understanding of the structure of apoC-I is therefore central to understanding its functional effects on the surface of lipoproteins.

ApoC-I, as a lipid-free monomer in solution, is largely unfolded exhibiting an average helical content of 31%.<sup>19,20</sup> The helical content increases to 65–75% in lipid-bound or self-associated states.<sup>20–22</sup> Nuclear magnetic resonance (NMR) and circular dichroism (CD) studies show that apoC-I contains four 11mer repeats, predicted to produce two lysine-rich class A

**Received:** September 29, 2011

**Revised:** January 19, 2012

**Published:** January 19, 2012

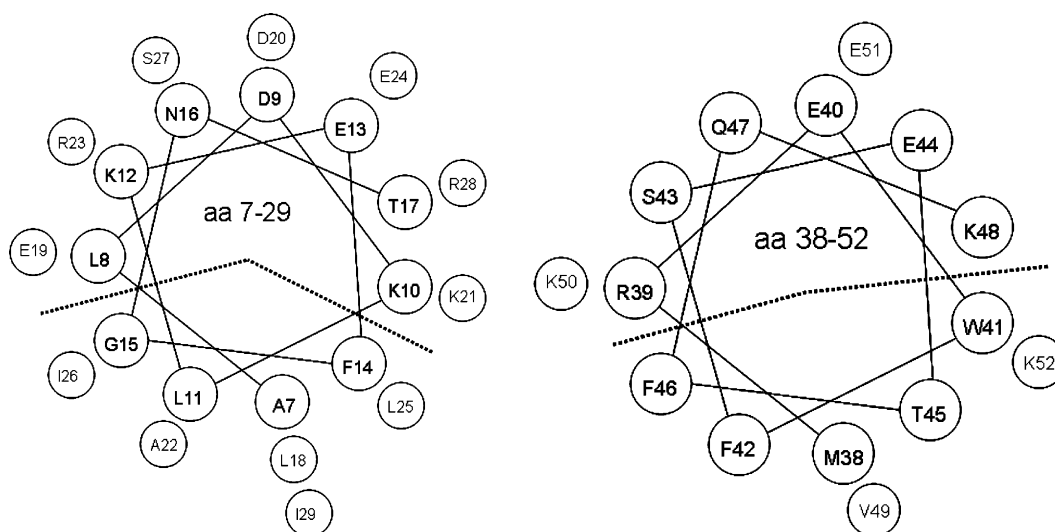


**Figure 1.** Helical wheel representation of the apoC-I  $\alpha$ -helices as  $\alpha 11/3$  helices. Hydrophobic helical faces are represented by dotted lines. The N-terminal A $\alpha$ H hydrophobic face (left) is comprised of nine residues (GLAFIALLI), and the C-terminal A $\alpha$ H hydrophobic face (right) is comprised of six residues (FFMTWV).

amphipathic  $\alpha$ -helices (A $\alpha$ H), spanning residues 7–29 and 38–52.<sup>23–28</sup> A common lipid surface-binding motif among apolipoproteins and synucleins, the class A A $\alpha$ H is characterized by a large (30–50%) apolar face essential for interactions with apolar lipid moieties and positive residues distributed in the polar–nonpolar interface, which interact with phospholipid headgroups and solvent molecules.<sup>29–33</sup>

Figure 1 depicts the N-terminal (left) and C-terminal (right) A $\alpha$ H helix wheel diagrams, with a dashed line demarcating their respective hydrophobic faces. The lysine residue (K52) at the end of the C-terminal A $\alpha$ H likely snorkels up out of the hydrophobic face.<sup>30,31</sup> Because of its structural similarity to apoA-I and  $\alpha$ -synuclein, apoC-I's A $\alpha$ Hs are modeled as  $\alpha 11/3$  helices.<sup>32,33</sup> Such helices are slightly unwound compared to the standard  $\alpha$ -helix, subsuming a rotation of 98.18° as opposed to 100° per residue.

To elucidate the interaction of apoC-I A $\alpha$ Hs with phospholipid on the lipoprotein surface, several studies monitored the effect of point mutations on binding of apoC-I to and stabilization of phospholipid vesicles.<sup>20,28,34–36</sup> Thermal denaturation and renaturation of apoC-I–DMPC complexes, monitored via CD, revealed the greatest reduction in apoC-I  $\alpha$ -helical content and the ability to reconstitute apoC-I–DMPC complexes for mutations interrupting the apolar face of either A $\alpha$ H.<sup>20,28</sup> These studies indicate an essential cooperativity in binding of the  $\alpha$ -helices to the phospholipid surface.<sup>20</sup> Additional studies, utilizing DMPC clearance assays and electron microscopy, showed that the C-terminal A $\alpha$ H contains aromatic residues essential for stabilizing the structure of the entire peptide and mediating phospholipid interactions.<sup>36</sup>

Apolipoprotein monolayers spread at an air/water (A/W) interface compared with apolipoprotein deposition at phospholipid/air/water (PL/A/W) interfaces provide additional insight into the interaction between apolipoproteins and phospholipid.<sup>37–43</sup> The surface pressure–area ( $\Pi$ –A) isotherms generated for compression of apoC-I monolayers at an A/W interface reveal a phase transition at a  $\Pi$  of ~37 mN/m and a collapse at a  $\Pi$  of ~47 mN/m.<sup>44,45</sup> Likewise, compression of apoC-I deposited on DPPC monolayers spread at an A/W interface revealed a phase transition beginning at a  $\Pi$  of ~24–

27 mN/m and a collapse at a  $\Pi$  of ~49 mN/m.<sup>46–48</sup> Brewster angle microscopy revealed that each phase transition could be attributed to different phases of apoC-I.<sup>44–48</sup> These results suggest a two-step desorption of apoC-I from A/W and DPPC/A/W interfaces, wherein one A $\alpha$ H desorbs at lower pressures ( $\Pi$  = 37 and 24–27 mN/m, respectively) before complete peptide desorption from the interface at higher pressures ( $\Pi$  = 47 and 49 mN/m, respectively).

Together, previous work with apoC-I and DMPC vesicles and apoC-I at a DPPC/A/W interface highlights the structural changes in apoC-I upon lipid binding and the conformational changes of the peptide as  $\Pi$  changes, which may happen in the transition of nascent HDL to mature, spherical HDL or of VLDL to LDL. Such studies are limited, however, by the lack of a truly physiologic interface, the ability to monitor quantitative, real-time surface modifications induced by apolipoprotein binding, and a full analysis of the effects of phospholipids on apolipoprotein binding.

To better ascertain how apolipoproteins change conformations or modify lipoprotein surfaces upon binding, the oil/water surface provides a model for peptide interactions with a TAG core, while a phospholipid/oil/water interface more closely resembles the lipoprotein surface. Both interfaces can be further refined by adding other molecules known to be in lipoprotein surfaces (e.g., cholesterol, fatty acids, etc.). To date, only a few studies<sup>37,49–55</sup> have examined the surface behavior of apolipoproteins or their consensus peptides at oil/water interfaces. Even fewer focused on the surface behavior of apolipoproteins at phospholipid/oil/water interfaces.<sup>56,57</sup>

In this study, we examined the interfacial properties of native apoC-I at TO/W and the more physiological palmitoyl-oleoyl-phosphatidylcholine/triolein/water (POPC/TO/W) interfaces. POPC better represents the phospholipid content at a lipoprotein surface than DMPC or DPPC, as POPC is found in abundance in TAG-rich lipoproteins, while DMPC and DPPC do not appear significantly on the surface of lipoproteins.<sup>57</sup> Our goal was to understand how apoC-I, via its amphipathic  $\alpha$ -helices, binds triacylglycerols (represented here by triolein) and/or phospholipids (POPC) and how

surface properties vary based on constituents on the modeled TO/PC surface.

To monitor the modifications induced by apoC-I at the lipoprotein surface, we used an oil-drop tensiometer<sup>53,58,59</sup> to measure and compare the adsorption isotherms, desorption behaviors, and elasticity properties of apoC-I at both interfaces. From this, we were able to see how interactions of the apoC-I A $\alpha$ H with POPC alter the binding of apoC-I to and its affinity for the interface. On the basis of the protocol of Mitsche et al.,<sup>57</sup> we varied the POPC surface concentration and quantitatively determined the effects on apoC-I surface retention as  $\Pi$  changes. From these results and comparison with other peptides we have studied, notably the A $\alpha$ H-rich apoA-I,<sup>52,55,57</sup> we propose a model in which apoC-I binds and increases  $\Pi$  to such a degree that molecules, such as apoE, HL, or CETP apolipoprotein activators, would be displaced from the surface.

## MATERIALS AND METHODS

**Materials.** Triolein (>99% pure) was purchased from NU-CHEK PREP, Inc. (Elysian, MN), and its interfacial tension ( $\gamma$ ) was 32 mN/m.

POPC (1-palmitoyl-2-oleoyl-*sn*-glycero-3-phosphocholine) was purchased from Avanti Polar Lipids (Alabaster, AL) dissolved in chloroform to a concentration of 25.0 mg/mL and stored at  $-20^{\circ}\text{C}$ . The POPC was dried under nitrogen and resuspended in 2 mM phosphate-buffered saline (PBS, pH 7.4) at a concentration of 2.5 or 5.0 mg/mL. Using a probe sonicator, the POPC in PBS was constituted into SUVs. POPC SUVs, using the method of Mitsche and Small,<sup>57</sup> were injected at varied concentrations into the aqueous phase and given sufficient time to adsorb to the preformed TO drop, such that the interfacial tension fell to 23–25 mN/m. At these  $\gamma$  values, roughly 42–37% of the TO drop was covered with POPC, based on calculations by Mitsche and Small.<sup>57</sup>

Full-size human apoC-I (57 amino acids) was obtained via solid-state synthesis and purified by high-performance liquid chromatography to 95–98% purity as described previously.<sup>20,28</sup> The N- and C-termini of the peptide were not blocked. SDS gels, CD, and electron microscopy revealed the structure and stability of wild-type (WT) apoC-I prepared by this method closely resemble those of the plasma protein (data not shown). A stock solution of peptide was made by adding 2 mM phosphate buffer (PB, pH 7.4) to a final peptide concentration of 1.0 mg/mL. Varied amounts of apoC-I stocks could be added to the aqueous phase to obtain different protein concentrations (from  $7.5 \times 10^{-8}$  to  $1 \times 10^{-6}$  M at a TO/W interface and from  $1 \times 10^{-7}$  to  $5 \times 10^{-7}$  M at a POPC/TO/W interface).

**Interfacial Tension ( $\gamma$ ) Measurement.** The interfacial tension ( $\gamma$ ) of TO/W and POPC/TO/W interfaces in the presence of varied concentrations of apoC-I in the aqueous phase was measured with an I. T. Concept (Longessaigne, France) Tracker oil-drop tensiometer,<sup>53,58,59</sup> with the goal of observing and quantifying the surface activity of apoC-I at either interface. A 16  $\mu\text{L}$  triolein drop was formed in 6.0 mL of gently stirred 2 mM PB (pH 7.4) containing no or varied concentrations of POPC. Varied amounts of apoC-I were added to the aqueous phase when TO/W interfaces had reached an equilibrium  $\gamma$  ( $\gamma_e$ ) of 32 mN/m or when POPC/TO/W interfaces had reached a  $\gamma$  between 23 and 25 mN/m. After POPC had adsorbed to the surface, the bulk buffer with POPC SUVs was exchanged with 250 mL of 2 mM POPC-free

PB (pH 7.4) prior to addition of apoC-I to the aqueous phase. This buffer exchange was done using the protocol of Mitsche and Small<sup>57</sup> and resulted in the removal of >99.9% of the original buffer. The  $\gamma$  of apoC-I at either interface was recorded continuously until it approached a  $\gamma_e$ . The surface pressure ( $\Pi$ ) was calculated from the surface tension of the TO/W interface ( $\gamma_{\text{TO}} = 32$  mN/m) minus the surface tension of the interface with POPC and apoC-I ( $\gamma$ ), such that  $\Pi = 32$  mN/m  $-\gamma$ . The temperature was  $25.0 \pm 0.1^{\circ}\text{C}$  for all experiments.

**Desorption and Readsorption Processes.** Following adsorption of apoC-I to either a TO/W or a POPC/TO/W interface, the drop underwent a series of compressions and re-expansions with the goal of determining if apoC-I completely or only partially desorbed from the respective interface. Once  $\gamma$  approached a  $\gamma_e$ , the TO drop (16  $\mu\text{L}$ ) was compressed by rapidly decreasing the volume by different ratios: 6.25% (1  $\mu\text{L}$ ), 12.5% (2  $\mu\text{L}$ ), 25% (4  $\mu\text{L}$ ), 37.5% (6  $\mu\text{L}$ ), 50% (8  $\mu\text{L}$ ), or, when possible, 62.5% (10  $\mu\text{L}$ ). This sudden decrease in volume induced a decrease in drop surface area, resulting in a sudden compression and abrupt decrease in  $\gamma$ . The oil drop was held at this reduced volume for 5–10 min, with  $\gamma$  recorded continuously. If apoC-I readily desorbed,  $\gamma$  increased to a  $\gamma_e$ , observed as a desorption curve. After 5–10 min, the interface was expanded by increasing the volume of the drop by equivalent ratios back to its initial volume (16  $\mu\text{L}$ ). As the surface area increased upon expansion,  $\gamma$  abruptly increased. If apoC-I adsorbed from the bulk phase and adhered to the newly formed extra surface,  $\gamma$  decreased to the initial  $\gamma_e$ , observed as a readsorption curve. This process of stress compression and re-expansion was repeated after the bulk buffer was exchanged with 150 mL of 2 mM PB (pH 7.4) devoid of apoC-I.

**Values of  $\Pi_{\text{max}}$ .** The desorption and readsorption protocol provided information about not only the nature of ejection of the peptide from either interface but also the  $\Pi$  at which such ejection occurs.  $\Pi_{\text{max}}$  is the maximal pressure ( $\Pi$ ) that a peptide can withstand before all or part of the molecule is ejected from the surface. Once a  $\gamma_e$  had been reached following adsorption of apoC-I to TO/W or POPC/TO/W interfaces, we conducted the series of experiments highlighted above in which the drop volume was decreased abruptly, thereby decreasing  $\gamma$  and increasing  $\Pi$  to a given value,  $\Pi_o$ . The change in tension ( $\Delta\gamma$ ) over the following 5–10 min as peptide desorbed from the surface was plotted against  $\Pi_o$ . Regression of a linear fit to the plot reveals  $\Pi_{\text{max}}$  as the point at which  $\Delta\gamma = 0$ , such that not even part of the peptide desorbs from the surface upon compression.<sup>51,52</sup>

**Equilibrium Oscillations of the Interface and the Elasticity Analysis.** Oscillating TO/W and POPC/TO/W interfaces with apoC-I bound allowed for comparison of viscoelasticity. After  $\gamma$  approached  $\gamma_e$  with apoC-I bound to either interface, the volume of the TO drop was oscillated sinusoidally at different periods ranging from 8 to 128 s and different amplitudes ranging from  $\pm 2$   $\mu\text{L}$  ( $\sim 13\%$ ) to  $\pm 8$   $\mu\text{L}$  (50%). As the volume oscillated, the interfacial area ( $A$ ) and surface tension ( $\gamma$ ) were recorded continuously. From these measurements of  $\gamma$  and  $A$ , pressure–area ( $\Pi$ – $A$ ) isotherms were derived and plotted, as  $\gamma = \Pi + 32.0$  mN/m. These measurements of  $\gamma$  and  $A$  also yielded the interfacial elasticity modulus, defined as  $\epsilon = d\gamma/d(\ln A)$ , for each sinusoidal oscillation.<sup>60</sup> Via Fourier transform analysis, the real [ $\epsilon' = |\epsilon| \cos(\varphi)$ ] and imaginary [ $\epsilon'' = |\epsilon| \sin(\varphi)$ ] components of  $\epsilon$  were determined, allowing for derivation of the phase angle ( $\varphi$ ) between compression and expansion. Increasing degrees of



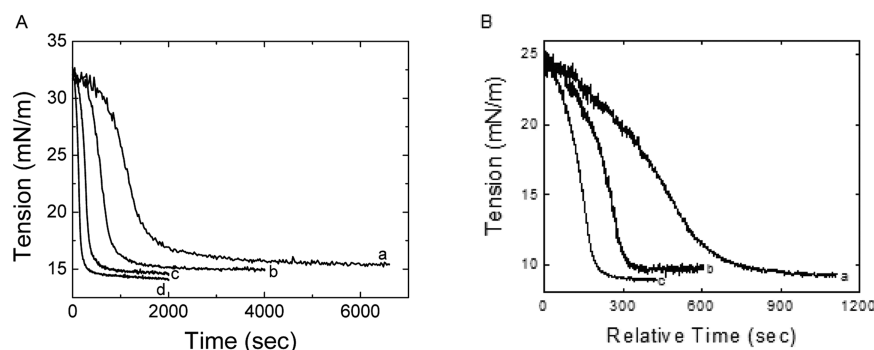


**Figure 2.** Plots of interfacial tension,  $\gamma$ , vs time of apoC-I at a TO/W interface (A) and a POPC/TO/W interface (B). A 16  $\mu\text{L}$  TO drop was formed in 2 mM PB (pH 7.4). (A) ApoC-I was added at varying concentrations: (a)  $7.5 \times 10^{-8}$ , (b)  $2.5 \times 10^{-7}$ , (c)  $5.0 \times 10^{-7}$ , and (d)  $1.0 \times 10^{-6}$  M. (B) POPC was adsorbed to the surface, and  $\gamma$  reached  $\sim 24$ – $25$  mN/m after buffer exchange. ApoC-I was added at relative time zero at varying concentrations. (a)  $1.0 \times 10^{-7}$ , (b)  $2.5 \times 10^{-7}$ , and (c)  $5.0 \times 10^{-7}$  M.

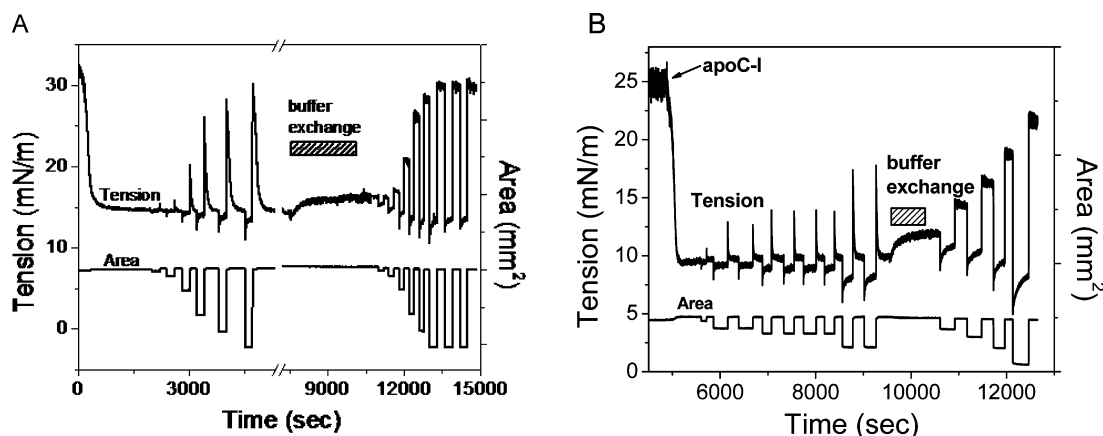


**Figure 3.** Desorption and readsorption curves of apoC-I at TO/W (A) and POPC/TO/W (B) interfaces. (A) A 16  $\mu\text{L}$  TO drop was compressed and subsequently re-expanded in increments of  $\pm 1$ ,  $\pm 2$ ,  $\pm 4$ ,  $\pm 6$ ,  $\pm 8$ , and  $\pm 10$   $\mu\text{L}$ . Following a 150 mL buffer exchange (shown by the bar), the drop was compressed and re-expanded in increments of  $\pm 1$ ,  $\pm 2$ ,  $\pm 4$ ,  $\pm 6$ ,  $\pm 8$ , and  $\pm 10$   $\mu\text{L}$  (three times). (B) A 16  $\mu\text{L}$  TO drop was compressed and re-expanded in increments of  $\pm 1$ ,  $\pm 2$  (two times),  $\pm 3$  (two times),  $\pm 4$  (two times), and  $\pm 6$   $\mu\text{L}$  (two times). Following a 150 mL buffer exchange (shown by the bar), the drop was compressed and re-expanded in increments of  $\pm 2$ ,  $\pm 4$ ,  $\pm 6$ , and  $\pm 8$   $\mu\text{L}$ . The apoC-I concentration in the aqueous phase was  $5.0 \times 10^{-7}$  M before and virtually zero after the buffer exchange for both panels A and B.

surface viscoelasticity are marked by decreasing  $\varepsilon$  and increasing  $\varphi$  values.

**Ramping Protocol and Corresponding  $\Pi$ –A Isotherms.** The goal of slowly expanding and sequentially compressing TO drops with apoC-I bound, but differing in POPC surface concentration ( $\Gamma_{\text{POPC}}$ ), was to quantitatively compare the point of compression at which apoC-I begins to be expelled from the POPC/TO/W interface. After adsorption of POPC to a TO/W interface lowered  $\gamma$  to 23–25.0 mN/m, the bulk buffer was exchanged with 250 mL of 2 mM POPC-free PB (pH 7.4), and  $\gamma$  was increased to 24.5–25.0 mN/m. The volume of the drop was then increased or decreased slowly ( $\pm 0.02$   $\mu\text{L/s}$ ), causing increases or decreases in  $\gamma$ . This resulted in corresponding decreases or increases in  $\Pi$ , respectively. The pressure of the interface ( $\Pi_i$ ) at which apoC-I was added could be correlated to  $\Gamma_{\text{POPC}}$ , and the equivalent percentage of POPC drop coverage, based on the work of Mitsche and Small.<sup>57</sup> Following adsorption of apoC-I to the POPC/TO/W interface lowering  $\gamma$  to a  $\gamma_e$ , the bulk buffer was exchanged with 150 mL of 2 mM PB (pH 7.4) devoid of apoC-I. The volume of the TO drop was then linearly increased at a rate of 0.02  $\mu\text{L/s}$  until the volume reached 30  $\mu\text{L}$ . After  $\gamma$  had been allowed to equilibrate for  $\geq 200$  s, the volume was linearly decreased at a rate of 0.02  $\mu\text{L/s}$  with the lower surface area limit varying, based on the

condition that  $\gamma$  remain above 5.0 mN/m. This protocol was repeated for several  $\Pi_i$  values, and pressure–area ( $\Pi$ –A) isotherms were calculated for each compression and expansion.

## RESULTS

**ApoC-I Is Surface Active and Binds to Triolein/Water (TO/W) and Palmitoylphosphatidylcholine/Triolein/Water (POPC/TO/W) Interfaces.** Changes in interfacial tension ( $\gamma$ ) upon injection of apoC-I into the aqueous phase reveal the peptide's surface activity at both TO/W and POPC/TO/W interfaces. Figure 2A shows a typical set of interfacial tension curves of the TO/W interface with varying concentrations of apoC-I in the aqueous phase. The initial  $\gamma$  of the TO/W interface was  $\sim 32$  mN/m. When varying concentrations of apoC-I were added to the aqueous phase ( $7.5 \times 10^{-8}$  to  $1.0 \times 10^{-6}$  M), the peptide adsorbed onto the TO/W interface, lowering  $\gamma$  and approaching a  $\gamma_e$ . At the lowest concentration ( $7.5 \times 10^{-8}$  M), a lag time of  $\sim 800$  s was observed before a sharp decrease in  $\gamma$  tapered into a gradual decrease approaching a  $\gamma_e$  between 1700 and 4000 s. As the apoC-I concentration increased, the lag period became shorter and the steepness of the rapid decrease in  $\gamma$  increased. Higher peptide concentrations also exhibited adsorption to lower  $\gamma_e$

values. The net changes in  $\gamma$  ranged from 16.5 mN/m ( $[\text{apoC-I}] = 7.5 \times 10^{-8} \text{ M}$ ) to 18.0 mN/m ( $[\text{apoC-I}] = 1.0 \times 10^{-6} \text{ M}$ ).

Figure 2B shows the set of interfacial tension curves of the POPC/TO/W interface with varying concentrations of apoC-I in the aqueous phase. The initial  $\gamma$  of the POPC/TO/W interface was  $\sim 24\text{--}25 \text{ mN/m}$ . Addition of apoC-I to the aqueous phase was chosen as relative time zero. The adsorption curves of apoC-I at this interface also showed three regions: a lag period during which  $\gamma$  decreased slowly with time, a second period with a faster decrease in  $\gamma$ , and a final period characterized by a gradual decrease in  $\gamma$  upon its approach to a  $\gamma_e$ . Similar to apoC-I at a TO/W interface, as the concentration of apoC-I increased at a POPC/TO/W interface, the lag period became shorter and the steepness of the rapid decrease in  $\gamma$  increased. Higher peptide concentrations did not, however, exhibit adsorption to lower  $\gamma_e$  values. Net changes in  $\gamma$  ranged from 15.5 mN/m ( $[\text{apoC-I}] = 1.0 \times 10^{-7} \text{ M}$ ) to 16 mN/m ( $[\text{apoC-I}] = 5.0 \times 10^{-7} \text{ M}$ ). These values are comparable to those for apoC-I at a TO/W interface. Consequently, apoC-I is surface active at both TO/W and POPC/TO/W interfaces, lowering interfacial tension in a similar manner and amount.

**ApoC-I Desorbs from TO/W and POPC/TO/W Interfaces on Compression.** Following adsorption of apoC-I to TO/ or POPC/TO/W interfaces, changes in  $\gamma$  induced by instantaneous compressions and subsequent expansions of the TO drop allow for determination of the nature of peptide desorption and readsorption. Figure 3A shows  $\gamma$  and area changes during the sudden compression and re-expansion of the TO/W interface for apoC-I before and after buffer exchange. After apoC-I adsorption lowered  $\gamma$  to a  $\gamma_e$  of  $\sim 15.0 \text{ mN/m}$ , the  $16 \mu\text{L}$  TO drop was compressed by decreasing its volume in increments varying from 1 to  $10 \mu\text{L}$ . This corresponded to area changes of 2–55%. Instantaneous decreases in  $\gamma$  increased with the size of compression. With a compression of  $4 \mu\text{L}$ ,  $\gamma$  decreased by  $\sim 2 \text{ mN/m}$ , while a compression of  $10 \mu\text{L}$  decreased  $\gamma$  by  $\sim 4 \text{ mN/m}$ .

When the compressed volume was held for several minutes,  $\gamma$  rose toward a  $\gamma_e$  slightly lower than the initial  $\gamma_e$ . This rise in  $\gamma$  indicates that peptide desorbs from the surface after instant compression. Because the new  $\gamma_e$  values are lower than  $15.0 \text{ mN/m}$ , particularly for larger compressions (Figure 3A), this indicates that bound apoC-I is compressed and potentially undergoes conformational rearrangement at the surface as  $\Pi$  increases. When the drop was re-expanded back to  $16 \mu\text{L}$ ,  $\gamma$  increased above the initial  $\gamma_e$ . Within a relatively short time ( $<60\text{s}$ ), however, peptide readsorbed and  $\gamma$  fell back to  $\sim 15.0 \text{ mN/m}$ , the initial  $\gamma_e$ .

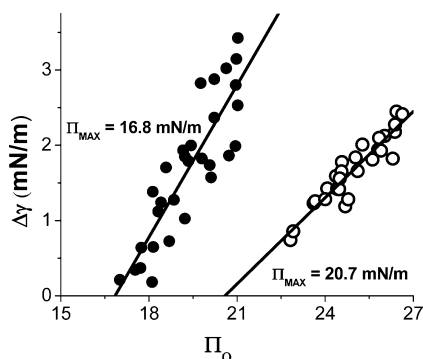
Buffer ( $150 \text{ mL}$ ) was exchanged (indicated by the bar in Figure 3A), and the apoC-I concentration was reduced to virtually zero.  $\gamma$  rose during the buffer exchange from  $\sim 15.0$  to  $\sim 17.0 \text{ mN/m}$ . This indicates that some bound apoC-I may desorb from the surface. The instant compression and expansion procedure was repeated with the TO drop (Figure 3A, right). A notable difference was that  $\gamma$  remained at or near heightened  $\gamma$  values following each re-expansion. If one A $\alpha$ H desorbed on compression and readily readsorbed on re-expansion,  $\gamma$  would decrease to a  $\gamma_e$  of  $\sim 17 \text{ mN/m}$ .  $\gamma$  would remain high following each re-expansion only if the entire peptide desorbed from the surface, with virtually no peptide molecules in the aqueous phase available to readsorb and lower  $\gamma$ .

Figure 3B shows  $\gamma$  and area changes during the sudden compression and expansion of apoC-I at the POPC/TO/W interface before and after buffer exchange. Upon POPC absorption,  $\gamma$  fell to  $23.2 \pm 0.1 \text{ mN/m}$ . A  $250 \text{ mL}$  buffer exchange caused  $\gamma$  to rise to  $25.0 \pm 0.3 \text{ mN/m}$ , because of exchange of POPC with the bulk solution. ApoC-I was added in the aqueous phase, and  $\gamma$  approached a  $\gamma_e$  of  $9.5 \pm 0.1 \text{ mN/m}$ . The TO drop was compressed by a decrease in its volume in increments ranging from 1 to  $6 \mu\text{L}$ , corresponding to area changes of 2–22%.

Similar to  $\gamma$  responses at the TO/W interface, each instant compression caused an instantaneous decrease in  $\gamma$ , but  $\gamma$  rose toward a new  $\gamma_e$  when the compressed volume was held for several minutes. The new  $\gamma_e$  values were lower than the initial  $\gamma_e$  of the interface. This can be most noticeably seen in the  $\gamma_e$  reached ( $8.1 \pm 0.2 \text{ mN/m}$ ) after the two  $6 \mu\text{L}$  compressions immediately preceding the buffer exchange in Figure 3B. This again indicates that apoC-I could undergo conformational rearrangement as its A $\alpha$ Hs are compressed as  $\Pi$  increases. After each re-expansion, apoC-I readsorption lowered  $\gamma$  to a  $\gamma_e$  similar to the initial  $\gamma_e$  ( $9.7 \pm 0.2 \text{ mN/m}$  in this case). This is preliminary evidence that apoC-I does not remove POPC when it desorbs from the POPC/TO/W interface. If apoC-I removed POPC as it desorbed upon compression,  $\gamma_e$  following re-expansion and readsorption of apoC-I would have risen to  $\sim 15.0 \text{ mN/m}$ , that of a POPC-free surface.

ApoC-I was removed from the aqueous phase by buffer exchange (indicated by the bar in Figure 3B), and  $\gamma_e$  rose to  $11.9 \pm 0.1 \text{ mN/m}$ , indicating that some apoC-I desorbs. An instant compression and expansion protocol similar to that before buffer exchange was repeated (Figure 3B, right). The POPC/TO/W interface, like the TO/W interface, did not relax back to  $\gamma_e$  levels after re-expansion but remained at or near the heightened  $\gamma$ . Consequently, at both interfaces, the entire apoC-I molecule is expelled upon compression and readsorbs when present in the bulk solution on re-expansion. Ejection of the entire peptide on compression is characteristic of exchangeable apolipoproteins.<sup>52,53,55,57</sup> The 44 N-terminal residues ([1–44]apoA-I) and 46 C-terminal residues ([198–243]apoA-I) of apoA-I are comprised of one and three A $\alpha$ Hs, respectively, and completely desorb from and readsorb to TO/W<sup>55</sup> and POPC/TO/W<sup>57</sup> interfaces.

**$\Pi_{\text{max}}$  Values for ApoC-I at TO/W and POPC/TO/W Interfaces.** Instant compression and re-expansion measurements were taken at different apoC-I concentrations to estimate the pressure ( $\Pi_{\text{max}}$ ) at which the entire peptide, as shown in Figure 3, is ejected from each interface. Differences in  $\Pi_{\text{max}}$  between the TO/W and POPC/TO/W interfaces would elucidate the role of apoC-I–POPC interactions in retention of the peptide on the lipoprotein surface. Because the initial pressure ( $\Pi_i$ ) at the POPC/TO/W interface prior to apoC-I adsorption was always  $\sim 7.0 \text{ mN/m}$  ( $\gamma_i = 25.0 \text{ mN/m}$ ) for these measurements, the  $\Pi_{\text{max}}$  value corresponds to a surface with roughly 38% POPC coverage. The data points shown in Figure 4 represent compression and re-expansion measurements prior to buffer exchange at both interfaces. Figure 4 shows that the  $\Pi_{\text{max}}$  of apoC-I at a TO/W interface is  $16.8 \text{ mN/m}$  (●) and the  $\Pi_{\text{max}}$  of apoC-I at a POPC/O/W interface is  $20.7 \text{ mN/m}$  (○). The greater  $\Pi_{\text{max}}$  of apoC-I at a POPC/TO/W interface suggests that apoC-I binds more strongly to a POPC/TO/W interface than a TO/W interface. Interactions of the apoC-I A $\alpha$ H with POPC likely increase its affinity for the interface.



**Figure 4.**  $\Pi_{\max}$  of apoC-I at the TO/W (●) and POPC/TO/W (○) interfaces. Each interface was instantly compressed to pressure  $\Pi_0$ . The  $\Delta\gamma$  while the compressed volume was held for several minutes was plotted vs  $\Pi_0$ . Linear regression of the data at each interface yielded intercepts at  $\Delta\gamma = 0$  equivalent to  $\Pi_{\max}$ , the pressure at which peptides show no net desorption or adsorption. The data shown for both interfaces represent mixed compression and expansion experiments after adsorption of varying concentrations of apoC-I, but before buffer exchange.

**Upon ApoC-I Adsorption, the POPC/TO/W Interface Shows Greater Elasticity Than the TO/W Interface.** The viscoelasticity of apoC-I at a TO/W or POPC/TO/W interface can be determined by oscillating either interface. Viscoelasticity represents a surface's ability to reduce deviations of  $\gamma$  from its equilibrium value by allowing for relaxation processes.<sup>60</sup> Typical relaxation processes consist of periodic adsorption and desorption of surface-active material (here, apoC-I) from expanded and compressed surface elements. This causes a change in the surface being compressed versus that being expanded in an oscillation shown as a hysteresis between the respective pressure–area ( $\Pi$ – $A$ ) isotherms.

Derived from the measurements of  $\gamma$  and  $A$  during oscillations, the elasticity modulus ( $\epsilon$ ) is defined as the increase in  $\gamma$  corresponding to a small increase in the area of a surface element [ $\epsilon = d\gamma/d(\ln A)$ ]. The phase angle ( $\phi$ ) represents the difference between the real and imaginary components of  $\epsilon$ . A higher  $\epsilon$  and lower  $\phi$ , therefore, indicate a surface more resistant to deformations or changes. If interactions of apoC-I with POPC retain the peptide at higher  $\Pi$  values, as indicated by a higher  $\Pi_{\max}$  (Figure 4), apoC-I should be more elastic at a

POPC/TO/W interface than at a TO/W interface. This would be marked by weaker hysteresis in oscillation  $\Pi$ – $A$  isotherms, greater  $\epsilon$  values, and lower  $\phi$  values.

Figure 5 shows  $\Pi$ – $A$  isotherms derived from equilibrium oscillations of apoC-I at TO/W (A) and POPC/TO/W (B) interfaces at different amplitudes and periods prior to buffer exchange. Two sets of  $\Pi$ – $A$  isotherms for apoC-I at a TO/W interface, each representing two or three periods for the given amplitude, are shown in Figure 5A. The  $\Pi$ – $A$  isotherms for apoC-I at a TO/W interface show significant hysteresis between compression and expansion when oscillated at larger amplitudes ( $\pm 8 \mu\text{L}$ ) and periods (32 and 128 s, represented by cyan and magenta lines, respectively). This indicates that sufficiently large changes in  $\Pi$  and sufficient time must be provided for observable desorption of apoC-I on compression.

The top half of Table 1 shows the  $\epsilon$  and  $\phi$  values calculated (as described in Materials and Methods) from the  $\Pi$ – $A$

**Table 1. Dynamic Interfacial Properties of ApoC-I at Different Interfaces<sup>a</sup>**

interface	[apoC-I] (M)	$V \pm \Delta V$ ( $\mu\text{L}$ )	period (s)	$\epsilon$ (mN/m)	$\phi$ (deg)
TO/W	$5.0 \times 10^{-7}$	$16 \pm 2$	8	29.6	10.6
		$16 \pm 2$	32	25.6	15.1
		$16 \pm 2$	128	20.4	23.5
		$16 \pm 8$	32	27.7	10.7
		$16 \pm 8$	128	25.6	12.3
POPC/TO/W	$1.0 \times 10^{-7}$	$18 \pm 2$	8	51.5	6.4
		$18 \pm 2$	32	51.2	7.8
		$18 \pm 2$	128	48.4	12.6
		$18 \pm 4$	8	47.7	6.0
		$18 \pm 4$	32	49.8	4.5
		$18 \pm 4$	128	48.9	7.6

<sup>a</sup>Analysis of the  $\Pi$ – $A$  oscillation isotherms sampled in Figure 5. Definitions: [apoC-I], concentration of apoC-I in the aqueous phase;  $V$ , initial drop volume;  $\Delta V$ , oscillation amplitude;  $\epsilon$ , elasticity modulus;  $\phi$ , phase angle, a phase difference between  $d\gamma$  and  $dA$ .

isotherms depicted in Figure 5A. Such analysis reveals  $\epsilon$  and  $\phi$  values at the TO/W interface ranging from 20.4 to 29.6 mN/m and from 10.6° to 23.5°, respectively, upon oscillations at amplitudes of  $\pm 2$  and  $\pm 8 \mu\text{L}$ . With increasing periods at a small

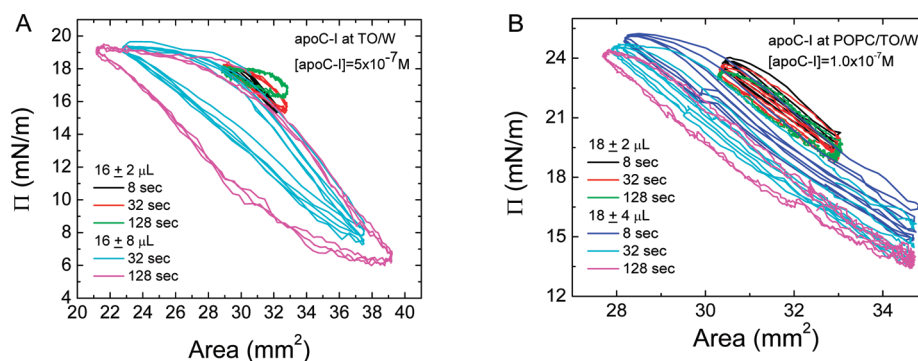


**Figure 5.** Plots of surface pressure ( $\Pi$ ) vs area for apoC-I at TO/W (A) and POPC/TO/W (B) interfaces derived from oscillations prior to buffer exchange. (A) After the  $\gamma_e$  for apoC-I at the TO/W interface had been reached, the  $16 \mu\text{L}$  TO drop was oscillated at  $16 \pm 2 \mu\text{L}$  ( $\Pi$  changes of approximately  $\pm 2$  mN/m) and  $16 \pm 8 \mu\text{L}$  ( $\Pi$  changes of approximately  $\pm 6.5$  mN/m) at periods of 8–128 s. The apoC-I concentration in the aqueous phase was  $5.0 \times 10^{-7}$  M. (B) After the  $\gamma_e$  for apoC-I at the POPC/TO/W interface had been reached, the volume of the TO drop was increased to  $18 \mu\text{L}$ . The drop was oscillated at  $18 \pm 2 \mu\text{L}$  ( $\Pi$  changes of approximately  $\pm 2.5$  mN/m) and  $18 \pm 4 \mu\text{L}$  ( $\Pi$  changes of approximately  $\pm 6$  mN/m) and periods of 8, 32, and 128 s. The apoC-I concentration in the aqueous phase was  $1.0 \times 10^{-7}$  M.



amplitude of  $\pm 2 \mu\text{L}$ ,  $\epsilon$  decreases by 9.2 mN/m and  $\phi$  increases by 12.9°. These significant changes reveal more apoC-I desorbs from and readsorbs to the surface with a greater oscillatory period, such that the surface is more viscoelastic.

Two sets of  $\Pi$ -A isotherms for apoC-I at a POPC/TO/W interface, each representing three periods for the given amplitude, are shown in Figure 5B. The  $\Pi$ -A isotherms for apoC-I at a POPC/TO/W interface show significantly less hysteresis between compression and expansion than those at a TO/W interface (Figure 5A). The lower half of Table 1, representing analysis of Figure 5B, reveals  $\epsilon$  and  $\phi$  values for the POPC/TO/W interface ranging from 48.4 to 51.5 mN/m and from 4.5° to 12.6°, respectively, at oscillation amplitudes of  $\pm 2$  and  $\pm 4 \mu\text{L}$ . Compared to those for a TO/W interface, these higher  $\epsilon$  and lower  $\phi$  values indicate apoC-I is more elastic at a POPC/TO/W interface. With increasing periods at a small amplitude of  $\pm 2 \mu\text{L}$ , the change in  $\epsilon$  is insignificant (3.1 mN/m) and  $\phi$  increases by 6.2°. Compared to those of a TO/W interface oscillated at the same amplitude, these changes are much smaller, indicating apoC-I binds with a higher affinity to a POPC/TO/W interface, creating a more elastic surface.

The small  $\phi$  and slight hysteresis in oscillations of apoC-I at a POPC/TO/W interface are indicative of a very small fraction of apoC-I, not POPC, desorbing from the interface. A series of control oscillations of the POPC/TO/W interface at varying initial  $\Pi$  values were performed over a wide range of amplitudes and periods (data not shown), and no hysteresis was observed, even for large amplitudes. This suggests that the interface is nearly completely elastic, such that there is no surface relaxation in which POPC desorbs and the lag between area changes and tension responses ( $\phi$ ) is nearly zero.<sup>60</sup>

**The Larger Percentage of POPC Coverage at the POPC/TO/W Interface Causes Greater Retention of ApoC-I upon Compression.** To determine the effect of varying  $\Gamma_{\text{POPC}}$  on surface retention of apoC-I, TO drops with apoC-I bound and increasing  $\Gamma_{\text{POPC}}$  underwent slow ( $\pm 0.02 \mu\text{L/s}$ ) expansions and subsequent compressions. This allows for quantitative comparison of the point on compression (the envelope point) at which apoC-I begins to be expelled from the POPC/TO/W interface. Figure 6 shows compression  $\Pi$ -A isotherms of the POPC/TO/W interface when apoC-I adsorbs to the POPC/TO/W interface at various initial interfacial tension values ( $\gamma_1$ ). Greater  $\gamma_1$  values correspond to a lower percentage of phospholipid coverage on the TO drop. Because  $\Pi = 32.0 \text{ mN/m} - \gamma$ , lower  $\Pi_1$  values correspond to lower POPC surface concentrations ( $\Gamma_{\text{POPC}}$ ) while higher  $\Pi_1$  values correspond to higher  $\Gamma_{\text{POPC}}$  values.<sup>37</sup> As listed in Table 2,  $\Pi_1$  values prior to apoC-I adsorption vary from 5.0 mN/m (31.8% of the drop is coated with POPC) in line a to 13.4 mN/m (51.8% of the drop is coated with POPC) in line d. Line e represents the  $\Pi$ -A compression isotherm for a POPC/TO/W interface devoid of apoC-I. As it does not overlap with the other compression isotherms, it shows that apoC-I adsorbed to and was being ejected from the POPC/TO/W interface in lines a–d.

In Figure 6, the envelope point (asterisk) represents the  $\Pi$  and A at which apoC-I begins to be ejected from the POPC/TO/W interface upon compression (direction indicated by an arrow). Visually, the envelope point is the point at which the slope of the compression isotherm dramatically decreases as area decreases. As  $\Gamma_{\text{POPC}}$  on the interface increases, the envelope point  $\Pi$  ( $\Pi_E$ ) increases, while the envelope point area ( $A_E$ ) decreases. As shown in Table 2,  $\Pi_E$  for apoC-I at the

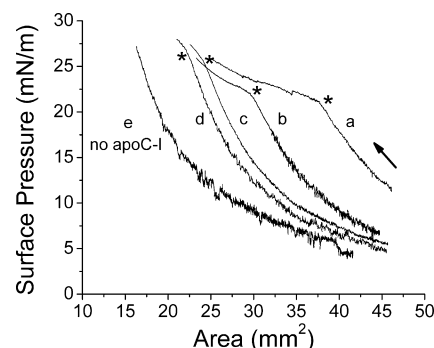


**Figure 6.** Pressure–area ( $\Pi$ -A) compression isotherms for apoC-I adsorbed to a POPC/TO/W interface at various initial  $\Pi$  values. ApoC-I, added at a concentration of  $2.5 \times 10^{-7} \text{ M}$  in the aqueous phase, adsorbed to POPC/TO/W interfaces at various initial pressures ( $\Pi_1$ ), listed for each curve in Table 2. After buffer exchange, each surface was slowly expanded and sequentially compressed. Shown here are compression isotherms, with the direction of compression marked by an arrow. Asterisks mark isotherm envelope points, where an abrupt change in slope indicates the beginning of ejection of apoC-I from the surface. Values of envelope pressure ( $\Pi_E$ ) and area ( $A_E$ ) for each curve are listed in Table 2. Line e represents the  $\Pi$ -A compression isotherm for the POPC/TO/W interface devoid of any apoC-I.

**Table 2. Envelope Pressures and Areas for ApoC-I at POPC/TO/W Interfaces with Increasing  $\Gamma_{\text{POPC}}$  Values<sup>a</sup>**

curve	$\Pi_1$ (mN/m)	$\Gamma_{\text{POPC}}$ (%)	$\Pi_E$ (mN/m)	$A_E$ (mm <sup>2</sup> )
a	$5.0 \pm 0.2$	$31.8 \pm 0.4$	$21.2 \pm 0.2$	$37.3 \pm 0.2$
b	$7.4 \pm 0.2$	$38.2 \pm 0.5$	$22.6 \pm 0.2$	$28.6 \pm 0.2$
c	$12.8 \pm 0.2$	$50.6 \pm 0.4$	$25.6 \pm 0.3$	$24.2 \pm 0.3$
d	$13.4 \pm 0.2$	$51.8 \pm 0.4$	$26.4 \pm 0.3$	$22.2 \pm 0.3$

<sup>a</sup>Analysis of the  $\Pi$ -A compression isotherms shown in Figure 6. Definitions:  $\Pi_1$ , initial pressure of the POPC/TO/W interface before apoC-I adsorption;  $\Gamma_{\text{POPC}}$ , initial POPC surface concentration before apoC-I adsorption, expressed as a percentage of total TO drop area;  $\Pi_E$  and  $A_E$ , envelope pressure and area, respectively, or the pressure and corresponding area, respectively, at which there is an abrupt change in the slope of the  $\Pi$ -A isotherm signifying ejection of apoC-I from the surface.

POPC/TO/W interface increases from 21.2 mN/m at the lowest  $\Gamma_{\text{POPC}}$  to 26.4 mN/m at the highest  $\Gamma_{\text{POPC}}$ . Conversely,  $A_E$  decreases by 15.1 mm<sup>2</sup> from 37.3 to 22.2 mm<sup>2</sup> over the same change in  $\Gamma_{\text{POPC}}$ . These data suggest that the higher the  $\Gamma_{\text{POPC}}$  on the POPC/TO/W interface, the greater the affinity of apoC-I for the interface and the more difficult it is to expel apoC-I from the surface. Consequently, apoC-I is retained up to higher pressures and smaller areas on the lipoprotein surface as  $\Gamma_{\text{POPC}}$  increases.

## DISCUSSION

On the surface of lipoproteins, it is reasonably assumed that apolipoproteins, including apoC-I, interact with phospholipids located on the surface.<sup>55</sup> It is also possible that apolipoproteins interact with core molecules, such as TAG or CE, notably when the number of surface lipid molecules is too small to adequately cover the core.<sup>55</sup> In this study, our goals were twofold. First, we sought to characterize the surface activity and reversible binding of human apoC-I at the TO/W interface and the more physiological POPC/TO/W interface. Second, we sought to understand the effects of interactions of apoC-I with POPC on

desorption of the peptide from and retention on the lipoprotein surface.

The first objective of this study was to demonstrate the surface activity of apoC-I at TO/W and POPC/TO/W interfaces. Figure 2 demonstrates the surface activity of apoC-I at both TO/W and POPC/TO/W interfaces. An increase in the rate of peptide adsorption was observed as the concentration of apoC-I in the aqueous phase increased. The decrease in  $\gamma$  (or increase in  $\Pi$ ) upon binding to each interface was comparable, equal to 16.5–18.0 or 15.5–16.0 mN/m, respectively. At a concentration of  $1.2 \times 10^{-6}$  M, similar to that of apoC-I used at a TO/W interface, [1–44]apoA-I and [198–243]apoA-I could increase  $\Pi$  by  $\sim 13.0$  mN/m at a TO/W interface.<sup>55</sup> This suggests a higher surface affinity for apoC-I than the C- and N-termini of apoA-I.

The observed surface affinity of apoC-I for either interface is imparted by its structure. Apolipoproteins exhibit strong lipid binding properties because of their characteristic secondary structures, containing amphipathic  $\alpha$ -helix (A $\alpha$ H) or amphipathic  $\beta$ -sheets (A $\beta$ S).<sup>29,49–53,61</sup> The lipid-binding motifs of apoC-I lie in its predicted N- and C-terminal A $\alpha$ Hs,<sup>25,28</sup> as shown in Figure 1. The hydrophobic face of each A $\alpha$ H (marked by a dotted line) is essential for interactions with apolar moieties on phospholipids (here, POPC) and neutral lipids (here, TO). According to the scale determined by Wimley and White,<sup>62</sup> the  $\Delta G_{b \rightarrow w}$  of partitioning for the hydrophobic face of the N-terminal A $\alpha$ H is 3.76 kcal/mol, or 0.42 kcal/mol per residue. The  $\Delta G_{b \rightarrow w}$  for the hydrophobic face of the C-terminal A $\alpha$ H is 4.13 kcal/mol, or 0.69 kcal/mol per residue. Preferential lipid binding is implicated in the unfavorable, positive  $\Delta G_{b \rightarrow w}$  of transfer from a bilayer interface to the aqueous phase for the hydrophobic faces of both A $\alpha$ Hs.

In association with its surface activity, we sought to determine the nature of binding of apoC-I to TO/W and POPC/TO/W interfaces. A $\alpha$ H structures typically show reversible binding to the TO/W surface, desorbing from and readsorbing to the surface upon compression and re-expansion.<sup>49,52,55</sup> Figure 3 reveals that apoC-I reversibly binds to both interfaces, desorbing when each interface is instantaneously compressed above  $\Pi_{\max}$ . ApoC-I's complete peptide desorption is evident in the  $\gamma$  responses of both interfaces for compression–expansion protocols after buffer exchange (right side of Figure 3A,B). With peptide present in the aqueous phase (Figures 3A,B), apoC-I readsorbs to both interfaces on re-expansion, decreasing  $\gamma$  to its initial equilibrium value (15.0 and 9.5 mN/m, respectively).

The left halves of panels A and B of Figure 3 suggest conformational rearrangement on compression of the A $\alpha$ Hs of apoC-I prior to complete peptide desorption at both interfaces, as the  $\gamma_e$  values reached after each compression are lower than the initial  $\gamma_e$ . The rise in  $\gamma$  at both interfaces due to the buffer exchange depicted in panels A and B of Figure 3 further suggests peptide conformational rearrangement at the surface, potentially followed by complete peptide desorption into the aqueous solution. To explain such conformational rearrangement, results of previous studies may suggest a two-step desorption model for apoC-I, with one A $\alpha$ H desorbing prior to complete peptide ejection.

Compression of apoC-I deposited on a DPPC monolayer at an A/W interface revealed two phase transitions.<sup>46–48,73</sup> The first occurs between  $\Pi$  values of 24 and 27 mN/m and the second at a  $\Pi$  of  $\sim 49$  mN/m. Brewster angle microscopy showed that only apoC-I was affected in each phase

transition.<sup>46–48</sup> This led to the proposal that, at  $\Pi$  values from 24 to 27 mN/m, one A $\alpha$ H on apoC-I desorbs from the subphase, aligning itself with the air, in a direction similar to that of the hydrophobic DPPC acyl chains.<sup>46,73</sup> The entire peptide was ejected from the monolayer at a  $\Pi$  of  $\sim 49$  mN/m.

Indicative of the order of apoC-I A $\alpha$ H desorption, the amide proton resonance line widths and deuterium exchange rates of the NMR structure of apoC-I–sodium dodecyl sulfate complexes suggest that the N-terminal A $\alpha$ H binds less tightly to the detergent than the C-terminal A $\alpha$ H.<sup>25</sup> In agreement with these results, James et al.<sup>36</sup> used mass spectrometry to show that the C-terminal region was the portion of apoC-I most highly protected from proteolysis. DMPC clearance assays and electron microscopy further revealed that single or double mutations in the apolar face of the C-terminal A $\alpha$ H of F42 and F46 to G or A result in a 2–3.5-fold reduction in the affinity of apoC-I for DMPC vesicles and apoC-I–DMPC complexes with atypical diameters.<sup>36</sup> However, CD studies of apoC-I–DMPC complexes show that interruptions in the apolar face of either the N-terminal (G15P) or C-terminal (T41P and T45P) A $\alpha$ H greatly reduce the level of protein–lipid binding.<sup>20,28</sup> Of all explored mutations, these also are the least able to reconstitute apoC-I–DMPC disks on thermal renaturation.<sup>20,28</sup> This indicates an essential cooperativity in binding of the  $\alpha$ -helices to the phospholipid surface.<sup>20</sup> The thermal denaturation and reconstitution of apoC-I–DMPC complexes, even at low ramp rates and small temperature changes, failed to show multiphase kinetics indicative of a two-step peptide desorption from the lipid–water interface.<sup>20,28,34,35</sup>

If apoC-I follows a two-step desorption from the lipoprotein surface, the NMR structure of apoC-I and greater  $\Delta G_{b \rightarrow w}$  values for the hydrophobic face of the C-terminal A $\alpha$ H predict that the N-terminal A $\alpha$ H desorbs prior to complete peptide desorption. Consequently, in the seconds following each instantaneous compression in Figure 3, the N-terminal A $\alpha$ H desorbs from the surface. This conversion is followed by a longer period of desorption of the C-terminal A $\alpha$ H of apoC-I to reach a new peptide equilibrium with the bulk solution.

Having characterized the reversible binding of apoC-I to TO/W and POPC/TO/W interfaces, we then sought to determine the effect of POPC on apoC-I surface binding and retention. To that end, pressure  $\Pi_{\max}$  at which the entire peptide begins to be ejected from TO/W and POPC/TO/W interfaces, was determined. Figure 4 reveals a  $\Pi_{\max}$  value of 16.8 mN/m for apoC-I at a TO/W interface. This  $\Pi_{\max}$  is consistent with previous findings for A $\alpha$ Hs at a TO/W interface, falling within the range of 13–19 mN/m.<sup>49,52,55</sup> Comparatively, the  $\Pi_{\max}$  values for [198–243]apoA-I and [1–44]apoA-I are 16.2 and 13.2 mN/m, respectively.<sup>55</sup>  $\Pi_{\max}$  for apoC-I at a POPC/TO/W interface depends on  $\Gamma_{\text{POPC}}$ . Figure 4 reveals that apoC-I has a  $\Pi_{\max}$  of 20.7 mN/m when  $\sim 38\%$  of the TO drop is covered by POPC. This higher  $\Pi_{\max}$  at a POPC/TO/W interface is likely caused by interactions of A $\alpha$ H with phospholipids and neutral lipids increasing the affinity of the peptide for the surface, keeping it bound at higher  $\Pi$  values.

The increase in the affinity for the interface induced by apoC-I–POPC interactions was further explored by sinusoidal oscillations of both interfaces following apoC-I adsorption. Figure 5 reveals the elastic properties of apoC-I at TO/W and POPC/TO/W interfaces. Previous studies have revealed that apoA-I, the major apolipoprotein constituent of HDL and primary activator of LCAT, binds TO/W interfaces via its A $\alpha$ H structural motifs and creates a highly flexible viscoelastic



interface.<sup>52</sup> Similarly, analysis of large oscillations or small oscillations with a slow period in Figure 5A reveals apoC-I forms a viscoelastic surface at the TO/W interface, marked by a large hysteresis in compression and expansion  $\Pi$ -A isotherms, a low  $\epsilon$ , and a large phase angle ( $\varphi$ ).

ApoC-I at a TO/W interface exhibits a marked hysteresis in its  $\Pi$ -A oscillation isotherms only at compressions of larger amplitudes and longer periods. This supports the two-step model of desorption of apoC-I from the interface, as ample time must be provided for the N-terminal A $\alpha$ H to desorb prior to complete peptide desorption. Oscillations with an amplitude of  $\pm 2 \mu\text{L}$  over a range of increasing periods yield  $\Pi$ -A isotherms for apoC-I at a TO/W interface with  $\varphi$  increasing by  $12.9^\circ$  from  $10.6^\circ$  to  $23.5^\circ$  and  $\epsilon$  decreasing by  $9.2 \text{ mN/m}$  from  $29.6$  to  $20.4 \text{ mN/m}$ .

Comparatively, the  $\Pi$ -A isotherms for apoC-I at a POPC/TO/W interface, oscillated over a range of amplitudes and periods, exhibit a much smaller hysteresis, even at larger amplitudes and longer periods. This is indicative of a more elastic interface. Oscillations with an amplitude of  $\pm 2 \mu\text{L}$  over a range of increasing periods yield  $\Pi$ -A isotherms for apoC-I at a POPC/TO/W interface with  $\varphi$  increasing by only  $6.2^\circ$  from  $6.4^\circ$  to  $12.6^\circ$  and  $\epsilon$  decreasing by only  $3.1 \text{ mN/m}$  from  $51.5$  to  $48.4 \text{ mN/m}$ . Compared to similar oscillations at a TO/W interface, these higher  $\epsilon$  and lower  $\varphi$  values are more resistant to change at a POPC/TO/W interface, which demonstrates a more elastic interface. These data indicate that interactions of the apoC-I A $\alpha$ H with POPC increase its affinity for and retention on the surface, thereby increasing surface elasticity.

To elucidate the role of A $\alpha$ H-phospholipid interactions on peptide retention at the lipoprotein surface, TO drops with apoC-I bound and increasing  $\Gamma_{\text{POPC}}$  values underwent slow expansions and subsequent compressions. Figure 6 and Table 2 show the dependency of the expulsion of apoC-I from the POPC/TO/W interface on the  $\Gamma_{\text{POPC}}$  of the TO drop. Increases in the  $\Gamma_{\text{POPC}}$  of the interface yield increases in  $\Pi_{\text{E}}$  and decreases in  $A_{\text{E}}$ , that is, the envelope pressure and area, respectively, at which apoC-I begins to be ejected from the interface. When POPC covers 32.8% of the TO drop surface (line a in Figure 6),  $\Pi_{\text{E}} = 21.2 \pm 0.2 \text{ mN/m}$  and  $A_{\text{E}} = 37.3 \pm 0.2 \text{ mm}^2$ , while at a POPC coverage of 51.8% (line d),  $\Pi_{\text{E}} = 26.4 \pm 0.3 \text{ mN/m}$  and  $A_{\text{E}} = 22.2 \pm 0.3 \text{ mm}^2$ . These results reveal that larger POPC:apoC-I ratios cause retention of apoC-I at higher  $\Pi$  values and more compact areas.

On the basis of the findings of this study, we propose possible mechanisms by which apoC-I may contribute to steps of lipoprotein remodeling, including CETP inhibition and prevention of hepatic uptake of TAG-rich lipoproteins. To inhibit CETP activity, the N-terminus of apoC-I could desorb from the lipoprotein surface, interacting with CETP and thereby interfering with its function.<sup>7,36</sup> With no discovered CETP-binding domain on apoC-I, a more likely mechanism of inhibition<sup>66</sup> is one in which apoC-I has a higher affinity for the lipoprotein surface than CETP or its activators: apolipoproteins A-I, A-II, A-IV, and E.<sup>63-67</sup> ApoA-IV has the weakest lipid affinity of any apolipoprotein,<sup>68,69</sup> and human C-apolipoproteins have been shown to displace apoA-IV from TAG-rich lipoprotein surfaces.<sup>69</sup> The C-terminus of apoA-I is predicted to be the most lipophilic portion of apoA-I, with the N-terminal helix bundle providing stability at the lipoprotein surface,<sup>70-72</sup> yet as shown, apoC-I causes greater changes in  $\Pi$  and has a higher  $\Pi_{\text{max}}$  than the C-terminus of apoA-I.<sup>55</sup> In this model of inhibition, apoC-I, at a sufficiently high plasma concentration,

could bind TAG-rich lipoproteins or compact HDL particles and drastically increase  $\Pi$ . These  $\Pi$  modifications could displace bound CETP and CETP activators or prevent them from binding.<sup>66</sup> Structurally similar to apoA-I, apoE could also be displaced from  $\beta$ -VLDL by apoC-I-induced  $\Pi$  modifications, thereby inhibiting lipoprotein uptake.<sup>16-18,72</sup>

In summary, our interfacial studies reveal that apoC-I is surface-active at both TO/W and POPC/TO/W interfaces, binding the interfaces via its two amphipathic  $\alpha$ -helices and lowering interfacial tension,  $\gamma$ . ApoC-I exhibits properties of an exchangeable apolipoprotein, desorbing upon compression and readsorbing upon re-expansion of either interface. Interactions of the A $\alpha$ H with POPC increase the affinity of apoC-I for the interface, demonstrated by a higher  $\Pi_{\text{max}}$  when roughly 38% of the interface was covered with POPC. Interactions of the A $\alpha$ H with POPC also increase surface elasticity, demonstrated by a higher elasticity modulus ( $\epsilon$ ), a lower phase angle ( $\varphi$ ), and reduced  $\Pi$ -A isotherm hysteresis during interface oscillation. Finally, the affinity of apoC-I for the POPC/TO/W interface increases as  $\Gamma_{\text{POPC}}$  increases, which is evident in higher envelope point  $\Pi$  values at lower envelope areas upon compression. We propose that the high-affinity binding of apoC-I to lipoprotein surfaces provides a possible model for inhibition of CETP activity by displacing or preventing the binding of its apolipoprotein activators. Similarly, the large changes in  $\Pi$  upon binding to triacylglycerol-rich lipoproteins could displace or prevent the binding of apoE to inhibit their receptor-mediated uptake.

## AUTHOR INFORMATION

### Corresponding Author

\*Department of Physiology and Biophysics, Boston University School of Medicine, 700 Albany St. W302, Boston, MA 02118-2526. Telephone: (617) 638-4002. Fax: (617) 638-4041. E-mail: dmsmall@bu.edu.

### Funding

This work was supported in part by National Heart, Lung and Blood Institute Grant 2P01 HL26335-21.

### Notes

The authors declare no competing financial interest.

## ACKNOWLEDGMENTS

We thank Dr. Olga Gursky for providing the human apolipoprotein C-I. We also thank Dr. Matt Mitsche for providing technical help and advice about the experimental protocol.

## ABBREVIATIONS

apoC-I, apolipoprotein C-I; HDL, high-density lipoprotein; VLDL, very-low-density lipoprotein; IDL, intermediate-density lipoprotein; LCAT, lecithin:cholesterol acyltransferase; CE, cholesterol ester; CETP, cholesterol ester transfer protein; LDL, low-density lipoprotein; TAG, triacylglycerol; HL, hepatic lipase; LPL, lipoprotein lipase; LRP, low-density lipoprotein receptor-related protein; A $\alpha$ H, amphipathic  $\alpha$ -helix; A/W, air/water; DPPC, dipalmitoylphosphatidylcholine; POPC, 1-palmitoyl-2-oleoylphosphatidylcholine; TO/W, triolein/water; PBS, phosphate-buffered saline; SUV, small unilamellar vesicle; [1-44]apoA-I, 44 N-terminal residues of apoA-I; [198-243]apoA-I, 46 C-terminal residues of apoA-I; A/ $\beta$ S, amphipathic  $\beta$ -sheet; DMPC, dimyristoylphosphatidylcholine; LDLR, LDL receptor; VLDLR, VLDL receptor.

# REFERENCES

- (1) Schaefer, E. J., Eisenberg, S., and Levy, R. I. (1978) Lipoprotein apoprotein metabolism. *J. Lipid Res.* 19 (6), 667–687.
- (2) Mahley, R. W., Innerarity, T. L., Rall, S. C., and Weisgraber, K. H. (1984) Plasma lipoproteins: Apolipoprotein structure and function. *J. Lipid Res.* 25 (12), 1277–1294.
- (3) Windler, E., and Havel, R. J. (1985) Inhibitory effects of C apolipoproteins from rats and humans on the uptake of triglyceride-rich lipoproteins and their remnants by the perfused rat liver. *J. Lipid Res.* 26 (5), 556–565.
- (4) Soutar, A. K., Garner, C. W., Baker, H. N., Sparrow, J. T., Jackson, R. L., Gotto, A. M., and Smith, L. C. (1975) Effect of the human plasma apolipoproteins and phosphatidylcholine acyl donor on the activity of lecithin:cholesterol acyltransferase. *Biochemistry* 14 (14), 3057–3064.
- (5) Jonas, A., Sweeny, S. A., and Herbert, P. N. (1984) Discoidal complexes of A and C apolipoproteins with lipids and their reactions with lecithin:cholesterol acyltransferase. *J. Biol. Chem.* 259 (10), 6369–6375.
- (6) Steyrer, E., and Kostner, G. M. (1988) Activation of lecithin-cholesterol acyltransferase by apolipoprotein D: Comparison of proteoliposomes containing apolipoprotein D, A-I, or C-I. *Biochim. Biophys. Acta* 958 (3), 484–491.
- (7) Gautier, T., Masson, D., Pais de Barros, J. P., Athias, A., Gambert, P., Aunis, D., Metz-Boutigue, M. H., and Lagrost, L. (2000) Human apolipoprotein C-I accounts for the ability of plasma high density lipoproteins to inhibit the cholesterol ester transfer protein activity. *J. Biol. Chem.* 275 (48), 37504–37509.
- (8) Masson, D., Pais de Barros, J. P., Zak, Z., Gautier, T., Le Guern, N., Assem, M., Chrisholm, J. W., Paterniti, J. R. Jr., and Lagrost, L. (2006) Human apoA-I expression in CETP transgenic rats leads to lower levels of apoC-I in HDL and to magnification of CETP-mediated lipoprotein changes. *J. Lipid Res.* 47 (2), 356–365.
- (9) Gautier, T., Tietge, U. J., Boverhof, R., Pertion, F. G., Le Guern, N., Masson, D., Rensen, P. C. N., Havekes, L. M., Lagrost, L., and Kuipers, F. (2007) Hepatic lipid accumulation in apolipoprotein C-I deficient mice is potentiated by cholesteryl ester transfer protein. *J. Lipid Res.* 48 (1), 30–40.
- (10) Kinnunen, P. K., and Ehnolm, C. (1976) Effect of serum and C-apoproteins from very low density lipoproteins on human postheparin plasma hepatic lipase. *FEBS Lett.* 65 (3), 354–357.
- (11) Conde-Knape, K., Bensadoun, A., Sobel, J. H., Cohn, J. S., and Shachter, N. S. (2002) Overexpression of apoC-I in apoE-null mice: Severe hypertriglyceridemia due to inhibition of hepatic lipase. *J. Lipid Res.* 43 (12), 2136–2145.
- (12) Rouhani, N., Young, E., Chatterjee, C., and Sparks, D. L. (2008) HDL composition regulates displacement of cell surface-bound hepatic lipase. *Lipids* 43 (9), 793–804.
- (13) Berbée, J. F. P., van der Hoogt, C. C., Sundararaman, D., Havekes, L. M., and Rensen, P. C. N. (2005) Severe hypertriglyceridemia in human APOC1 transgenic mice is caused by apoC-I-induced inhibition of LPL. *J. Lipid Res.* 46 (2), 297–306.
- (14) Jong, M. C., Gijbels, M. J., Dahlmans, V. E., Gorp, P. J., Koopman, S. J., Ponc, M., Hofker, M. H., and Havekes, L. M. (1998) Hyperlipidemia and cutaneous abnormalities in transgenic mice overexpressing human apolipoprotein C1. *J. Clin. Invest.* 101 (1), 145–152.
- (15) Shachter, N. S., Ebara, T., Ramakrishnan, R., Steiner, G., Breslow, J. L., Ginsberg, H. N., and Smith, J. D. (1996) Combined hyperlipidemia in transgenic mice overexpressing human apolipoprotein C1. *J. Clin. Invest.* 98 (3), 846–855.
- (16) Weisgraber, K. H., Mahley, R. W., Kowal, R. C., Herz, J., Goldstein, J. L., and Brown, M. S. (1990) Apolipoprotein C-I modulates the interaction of apolipoprotein E with  $\beta$ -migrating very low density lipoproteins ( $\beta$ -VLDL) and inhibits binding of  $\beta$ -VLDL to low density lipoprotein receptor-related protein. *J. Biol. Chem.* 265 (36), 22453–22459.
- (17) Sehaye, E., and Eisenberg, S. (1991) Mechanisms of inhibition by apolipoprotein C of apolipoprotein E-dependent cellular metabolism of human triglyceride-rich lipoproteins through the low density lipoprotein receptor pathway. *J. Biol. Chem.* 266 (27), 18259–18267.
- (18) Nestel, P. J., and Fidge, N. H. (1982) Apo C metabolism in man. *Adv. Lipid Res.* 19, 55–83.
- (19) Gursky, O., and Atkinson, D. (1998) Thermodynamic analysis of human plasma apolipoprotein C-I: High-temperature unfolding and low-temperature oligomer dissociation. *Biochemistry* 37 (5), 1283–1291.
- (20) Benjwal, S., Jayaraman, S., and Gursky, O. (2007) Role of secondary structure in protein-phospholipid surface interactions: Reconstitution and denaturation of apolipoprotein C-DMPC complexes. *Biochemistry* 46 (13), 4184–4194.
- (21) Osborne, J. C. Jr., Bronzert, T. J., and Brewer, H. B. Jr. (1977) Self-association of apo-C-I from the human high density lipoprotein complex. *J. Biol. Chem.* 252 (16), 5756–5760.
- (22) Osborne, J. C. Jr., Lee, N. S., and Powell, G. M. (1986) Solution properties of apolipoproteins. *Methods Enzymol.* 128, 375–387.
- (23) Jackson, R. L., Sparrow, J. T., Baker, H. N., Morrisett, J. D., Taunton, O. D., and Gotto, A. M. Jr. (1974) The primary structure of apolipoprotein-serine. *J. Biol. Chem.* 249 (16), 5308–5313.
- (24) Shulman, R. S., Herbert, P. N., Wehrly, K., and Fredrickson, D. S. (1975) The complete amino acid sequence of C-I (apoLP-Ser), an apolipoprotein from human very low density lipoproteins. *J. Biol. Chem.* 250 (1), 182–190.
- (25) Rozek, A., Sparrow, J. T., Weisgraber, K. H., and Cushley, R. J. (1999) Conformation of human apolipoprotein C-I in a lipid-mimetic environment determined by CD and NMR spectroscopy. *Biochemistry* 38 (44), 14475–14484.
- (26) Rozek, A., Buchko, G. W., and Cushley, R. J. (1995) Conformation of two peptides corresponding to human apolipoprotein C-I residues 7–24 and 35–53 in the presence of sodium dodecyl sulfate by CD and NMR spectroscopy. *Biochemistry* 34 (22), 7401–7408.
- (27) Rozek, A., Buchko, G. W., Kanda, P., and Cushley, R. J. (1997) Conformational studies of the N-terminal lipid-associating domain of human apolipoprotein C-I by CD and <sup>1</sup>H NMR spectroscopy. *Protein Sci.* 6 (9), 1858–1868.
- (28) Gursky, O. (2001) Solution conformation of human apolipoprotein C-I inferred from proline mutagenesis: Far- and near-UV CD study. *Biochemistry* 40 (40), 12178–12185.
- (29) Segrest, J. P., Jones, M. K., DeLoof, H., Brouillette, C. G., Venkatachalapathi, Y. V., and Anantharamaiah, G. M. (1992) The amphipathic helix in the exchangeable apolipoproteins: A review of secondary structure and function. *J. Lipid Res.* 33 (2), 141–166.
- (30) Segrest, J. P., DeLoof, H., Dohlman, J. G., Brouillette, C. G., and Anantharamaiah, G. M. (1990) Amphipathic helix motif: Classes and properties. *Proteins* 8 (2), 103–117.
- (31) Mishra, V. K., Palgunachari, M. N., Segrest, J. P., and Anantharamaiah, G. M. (1994) Interactions of synthetic peptide analogs of the class A amphipathic helix with lipids. Evidence for the snorkel hypothesis. *J. Biol. Chem.* 269 (10), 7185–7191.
- (32) Segrest, J. P., Jones, M. K., Klon, A. E., Sheldahl, C. J., Hellinger, M., De Loof, H., and Harvey, S. C. (1999) A detailed molecular belt model for human apolipoprotein A-I in discoidal high density lipoprotein. *J. Biol. Chem.* 274 (45), 31755–31758.
- (33) Bussell, R. Jr., and Eliezer, D. (2003) A structural and functional role for 11-mer repeats in  $\alpha$  synuclein and other exchangeable lipid binding proteins. *J. Mol. Biol.* 329 (4), 763–778.
- (34) Gursky, O., Mehta, R., and Gantz, D. L. (2002) Complex of human apolipoprotein C-I with phospholipid: Thermodynamic or kinetic stability. *Biochemistry* 41 (23), 7373–7384.
- (35) Mehta, R., Gantz, D. L., and Gursky, O. (2003) Effects of mutations in apolipoprotein C-I on the reconstitution and kinetic stability of discoidal lipoproteins. *Biochemistry* 42 (16), 4751–4758.
- (36) James, P. F., Dogovski, C., Dobson, R. C. J., Bailey, M. F., Goldie, K. N., Karas, J. A., Scanlon, D. B., O'Hair, R. A. J., and Perugini, M. A. (2009) Aromatic residues in the C-terminal helix on

human apoC-I mediate phospholipid interactions and particle morphology. *J. Lipid Res.* 50 (7), 1384–1394.

(37) Weinberg, R. B., Cook, V. R., DeLozier, J. A., and Shelness, G. S. (2000) Dynamic interfacial properties of human apolipoproteins A-IV and B-17 at the air/water and oil/water interface. *J. Lipid Res.* 41 (9), 1419–1427.

(38) Phillips, M. C., and Krebs, K. E. (1986) Studies of apolipoproteins at the air/water interface. *Methods Enzymol.* 128, 387–403.

(39) Krebs, K. E., Phillips, M. C., and Sparkes, C. E. (1983) A comparison of the surface activities of rat plasma apolipoproteins C-II, C-III-0, C-III-3. *Biochim. Biophys. Acta* 751 (3), 470–473.

(40) Ibdah, J. A., and Phillips, M. C. (1988) Effects on lipid composition and packing on the adsorption of apolipoprotein A-I to lipid monolayers. *Biochemistry* 27 (18), 7155–7162.

(41) Ibdah, J. A., Lund-Katz, S., and Phillips, M. C. (1989) Molecular packing of high-density and low-density lipoprotein surface lipids and apolipoprotein A-I binding. *Biochemistry* 28 (3), 1126–1133.

(42) Ibdah, J. A., Krebs, K. E., and Phillips, M. C. (1989) The surface properties of apolipoproteins A-I and A-II at the lipid/water interface. *Biochim. Biophys. Acta* 1004 (3), 300–308.

(43) Weinberg, R. B., Ibdah, J. A., and Phillips, M. C. (1992) Adsorption of apolipoprotein A-IV to phospholipid monolayers spread at the air/water interface. A model for its labile binding to high density lipoproteins. *J. Biol. Chem.* 267 (13), 8977–8983.

(44) Bolaños-García, V. M., Mas-Oliva, J., Ramos, S., and Castillo, R. (1999) Phase transitions in monolayers of human apolipoprotein C-I. *J. Phys. Chem. B* 103, 6236–6242.

(45) Bolaños-García, V. M., Ramos, S., Xicohtencatl-Cortés, J., Castillo, R., and Mas-Oliva, J. (2001) Monolayers of apolipoproteins at the air/water interface. *J. Phys. Chem. B* 105, 5757–5765.

(46) Xicohtencatl-Cortés, J., Mas-Oliva, J., and Castillo, R. (2004) Phase transitions of phospholipid monolayers penetrated by apolipoproteins. *J. Phys. Chem. B* 108 (22), 7307–7315.

(47) Xicohtencatl-Cortés, J., Castillo, R., and Mas-Oliva, J. (2004) In search of new structural states of exchangeable apolipoproteins. *Biochem. Biophys. Res. Commun.* 324 (2), 467–470.

(48) Mendoza-Espinosa, P., Moreno, A., Castillo, R., and Mas-Oliva, J. (2008) Lipid dependent disorder-to-order conformational transitions in apolipoprotein CI derived peptides. *Biochem. Biophys. Res. Commun.* 365, 8–15.

(49) Wang, L., Atkinson, D., and Small, D. M. (2003) Interfacial properties of an amphipathic  $\alpha$ -helix consensus peptide of exchangeable apolipoproteins at air/water and oil/water interfaces. *J. Biol. Chem.* 278 (39), 37480–37491.

(50) Wang, L., and Small, D. M. (2004) Interfacial properties of amphipathic  $\beta$  strand consensus peptides of apolipoprotein B at oil/water interfaces. *J. Lipid Res.* 45 (9), 1704–1715.

(51) Wang, L., Jiang, Z. G., McKnight, C. J., and Small, D. M. (2010) Interfacial properties of apolipoprotein B292–593 (B 6.4–13) and B611–782 (B 13–17). Insights into the structure of the lipovitellin homology region in apolipoprotein B. *Biochemistry* 49 (18), 3898–3907.

(52) Wang, L., Atkinson, D., and Small, D. M. (2005) The interfacial properties of apoA-I and an amphipathic  $\alpha$ -helix consensus peptide of exchangeable apolipoproteins at the triolein/water interface. *J. Biol. Chem.* 280 (6), 4154–4165.

(53) Small, D. M., Wang, L., and Mitsche, M. A. (2009) The adsorption of biological peptides and proteins at the oil/water interface. A potentially important but largely unexplored field. *J. Lipid Res.* No. April Suppl., S329–S334.

(54) Mitsche, M. A., Wang, L., Jiang, Z. G., McKnight, C. J., and Small, D. M. (2009) Interfacial properties of a complex multi-domain 490 amino acid peptide derived from apolipoprotein B (residues 292–782). *Langmuir* 25 (4), 2322–2330.

(55) Wang, L., Hua, N., Atkinson, D., and Small, D. M. (2007) The N-terminal (1–44) and C-terminal (198–243) peptides of apolipoprotein A-I behave differently at the triolein/water interface. *Biochemistry* 46 (43), 12140–12151.

(56) Ledford, A. S., Cook, V. A., Shelness, G. S., and Weinberg, R. B. (2009) Structural and dynamic interfacial properties of the lipoprotein initiating domain of apolipoprotein B. *J. Lipid Res.* 50 (1), 108–115.

(57) Mitsche, M. A., and Small, D. M. (2011) C-terminus of apolipoprotein A-I removes phospholipid from a triolein/phospholipids/water interface, but the N-terminus does not: A possible mechanism for nascent HDL assembly. *Biophys. J.* 101 (2), 353–361.

(58) Labourdenne, S., Gaudry-Rolland, N., Letellier, S., Lin, M., Cagna, A., Esposito, G., Verger, R., and Rivi re, C. (1994) The oil-drop tensiometer: Potential applications for studying the kinetics of (phospho) lipase action. *Chem. Phys. Lipids* 71 (2), 163–173.

(59) Mitsche, M. A., Wang, L., and Small, D. M. (2010) Adsorption of egg phosphatidylcholine to an air/water and triolein/water bubble interface: Use of the 2-dimensional phase rule to estimate the surface composition of a phospholipid/triolein/water surface as a function of surface pressure. *J. Phys. Chem. B* 114 (9), 3276–3284.

(60) Lucassen, J., and Van den Tempel, M. (1972) Dynamic measurements of dilational properties of a liquid interface. *Chem. Eng. Sci.* 27, 1283–1291.

(61) Segrest, J. P., Jones, M. K., De Loof, H., and Dashti, N. (2001) Structure of apolipoprotein B-100 in low density lipoproteins. *J. Lipid Res.* 42 (9), 1346–1367.

(62) Wimley, W. C., and White, S. H. (1996) Experimentally determined hydrophobicity scale for proteins at membrane interfaces. *Nat. Struct. Biol.* 3, 842–848.

(63) Main, L. A., Ohnishi, T., and Yokoyama, S. (1996) Activation of human plasma cholesteryl ester transfer protein by human apolipoprotein A-IV. *Biochim. Biophys. Acta* 1300 (1), 17–24.

(64) Milner, T. G., Ko, K. W. S., Ohnishi, T., and Yokoyama, S. (1991) Enhancement of the human plasma lipid transfer protein reaction by apolipoproteins. *Biochim. Biophys. Acta* 1082 (1), 71–78.

(65) Ohnishi, T., and Yokoyama, S. (1993) Activation of human plasma lipid transfer protein by apolipoproteins. *Biochemistry* 32 (19), 5029–5035.

(66) Weinberg, R. B., Anderson, R. A., Cook, V. R., Emmanuel, F., Den fle, P., Tall, A. R., and Steinmetz, A. (2002) Interfacial exclusion pressure determines the ability of apolipoprotein A-IV truncation mutants to activate cholesterol ester transfer protein. *J. Biol. Chem.* 277 (24), 21549–21553.

(67) Guyard-Dangremont, V., Lagrost, L., and Gambert, P. (1994) Comparative effects of purified apolipoproteins A-I, A-II, and A-IV on cholesteryl ester transfer protein activity. *J. Lipid Res.* 35 (6), 982–992.

(68) Weinberg, R. B., and Jordan, M. (1990) Effects of phospholipid on the structure of human apolipoprotein A-IV. *J. Biol. Chem.* 265 (14), 8081–8086.

(69) Weinberg, R. B., and Spector, M. S. (1985) Human apolipoprotein A-IV: Displacement from the surface of triglyceride-rich particles by HDL2-associated C-apoproteins. *J. Lipid Res.* 26 (1), 26–37.

(70) Laccotripe, M., Makrides, S. C., Jonas, A., and Zannis, V. I. (1998) The carboxyl-terminal hydrophobic residues of apolipoprotein A-I affect its rate of phospholipid binding and its association with high density lipoprotein. *J. Biol. Chem.* 272 (28), 17511–17522.

(71) Lyssenko, N. N., Hata, M., Dhanasekaran, P., Nickel, M., Nguyen, D., Chetty, P. S., Saito, H., Lund-Katz, S., and Phillips, M. C. (2011) Influence of C-terminal  $\alpha$ -helix hydrophobicity and aromatic amino acid content on apolipoprotein A-I functionality. *Biochim. Biophys. Acta*, [Epub ahead of print].

(72) Saito, H., Dhanasekaran, P., Nguyen, D., Holvoet, P., Lund-Katz, S., and Phillips, M. C. (2003) Domain structure and lipid interaction in human apolipoproteins A-I and E, a general model. *J. Biol. Chem.* 278 (26), 23227–23232.

(73) Bolaños-García, V. M., Renault, A., and Beaufils, S. (2008) Surface rheology and adsorption kinetics reveal the relative amphiphilicity, interfacial activity, and stability of human exchangeable apolipoproteins. *Biophys. J.* 94 (5), 1735–1745.